

# Six Principal Modes of Vibrotactile Display via Stylus

Ruisi Zhang, Andrew J. Boyles, and Jake J. Abbott

**Abstract**—Vibrotactile display can significantly enhance the haptic fidelity of tool-mediated interaction with virtual surfaces. Although there has been significant research on this topic, there is little known about vibrotactile perception when using torque-based actuation, nor how it is perceived in comparison to force-based actuation. This study characterizes the vibrotactile detection thresholds in the frequency range of 20–250 Hz of ten human subjects holding a stylus with a precision grasp. For the first time, we consider all six principal modes of vibrotactile display rendered at the haptic interaction point of the stylus, which includes three orthogonal force directions and three orthogonal torque directions. We find that subjects are far more sensitive to torque signals about the shaft of the stylus than to torque signals orthogonal to the shaft. We find that, at low frequencies, subjects are less sensitive to force signals parallel to the shaft of the stylus than to force signals orthogonal to the shaft. We find that the thresholds for force and torque signals applied orthogonal to the shaft of the stylus can be approximately equated by considering the reaction moment felt at the grasp point, which enables all six principal modes to be quantitatively compared.

## I. INTRODUCTION

By rendering high-frequency vibrations, haptic interfaces can significantly enhance the vibrotactile perception illusion of touching a real surface in virtual environments [1]. In particular, the ability to render texture is important in surgical simulators and training systems, which motivates much of the research in the field of haptics [2]. Understanding vibrotactile display via tool-mediated contact using a precision grasp is particularly important, since this is the most common way to manipulate a medical tool [3]. We are particularly interested in the use of untethered magnetic haptic interfaces in this context [4]. However, although there has been significant research on the topic of vibrotactile display [5], there is little known about vibrotactile perception using torque signals with precision grasp (about any axis), nor how they are perceived in comparison to force signals (which have been characterized only for vibrations along the stylus [6]).

In this paper, we perform a psychophysical study to measure the vibrotactile detection thresholds for a stylus held with a precision grasp, for the range of frequencies of interest for vibrotactile display (20–250 Hz), in each of the six principal modes: three orthogonal force directions and three orthogonal torque directions, applied in a standard coordinate frame located at the point on the stylus where force and torque are rendered, i.e., the haptic interaction

point (HIP). The response variable quantifying threshold is the amplitude of the sinusoidal force or torque signal.

During vibrotactile display using a stylus with a precision grasp, multiple contact points between the hand and the stylus are vibrated simultaneously. The mechanoreceptors in the glabrous finger skin respond to vibrations from all directions, but humans themselves cannot distinguish the direction of the vibration [7]. In addition, the measured mechanical impedance of the skin of the hand, using locally applied small-amplitude sinusoidal vibrations, showed no difference between vibrations applied parallel and perpendicular to the skin surface [8]. Modern haptic studies considering vibrotactile display via stylus using a precision grasp typically assume that humans perceive the same intensity of vibrotactile stimuli in every direction [9], [10], which has resulted in the attachment of the vibrotactile actuators in orientations that may not correspond to the direction in which users are most sensitive. Brisben et al. [11] suggest that vibrations parallel to the skin surface could be easier to detect than vibrations perpendicular to the skin surface when using a power grasp. However, the power grasp involves a large area of the palm and fingers, whereas the precision grasp involves a substantially different and smaller area of the hand [3], which, when combined with the fact that humans' palms are more sensitive than the fingers [11], suggests that directly applying Brisben's conclusion might be inappropriate for precision grasp. Our study considers precision grasp holistically, without any preconceived notions about the relative sensations between the stimuli applied in the six principal modes.

In our study, we use an untethered magnetic haptic interface comprising an electromagnetic field-generation source and a fully untethered stylus that has a permanent magnet attached at one end, the center of which serves as the HIP [4]. Our interface is capable of rendering vibrotactile sensations in each of the six principal modes, independently, with a single stylus (i.e., with no change to the inertia of the stylus), making it ideal for this study. Untethered magnetic haptic interfaces differ from traditional haptic interfaces that utilize one or more vibrotactile actuators to render vibrations [5]. A vibrotactile actuator can only render one-dimensional vibration, driven by either force or torque, making it challenging to render independent vibrations in different directions while controlling for actuation authority and stylus inertial properties. Although our experiment uses an untethered magnetic haptic interface, the results of our study will generalize to any haptic interface using a stylus of similar size, provided the actuation applied at the HIP is a force or torque (i.e., the interface is “impedance-type”).

This work was supported by the National Science Foundation under grant number 1423273.

The authors are with the Department of Mechanical Engineering and the Robotics Center, University of Utah, USA. A. J. Boyles is now with the Department of Mechanical Engineering, University of California, Santa Barbara, USA. [ruisi.zhang@utah.edu](mailto:ruisi.zhang@utah.edu)

## II. METHODS

### A. Subjects

The study is performed by ten (five male, five female) right-handed subjects, whose ages range from 23 to 31 years. Subjects have normal tactile sensation and normal (corrected) vision, by self-report. The study was approved by the University of Utah Institutional Review Board.

### B. Apparatus

The custom untethered magnetic haptic interface (Fig. 1) comprises two separate parts: an electromagnetic field source known as an Omnimagnet, and an untethered stylus with a cubic permanent magnet rigidly attached to one end.

An Omnimagnet [12] comprises three mutually orthogonal nested coils with a spherical ferromagnetic core in the center, with a design that was optimized to maximize the accuracy of the dipole field model as a description of its field:

$$\mathbf{b}(\mathbf{p}) = \frac{\mu_0}{4\pi\|\mathbf{p}\|^5} (3\mathbf{p}\mathbf{p}^T - \|\mathbf{p}\|^2\mathbf{I}) \mathbf{M}$$

where  $\mathbf{M}$  is the dipole moment of the Omnimagnet,  $\mathbf{p}$  is a point measured from the center of the Omnimagnet,  $\mu_0$  is the permeability of free space,  $\mathbf{I}$  is the identity matrix, and  $\mathbf{b}$  is the resulting magnetic field vector (i.e., magnetic flux density) at  $\mathbf{p}$ . The specific Omnimagnet used is one of the “small” Omnimagnets described in [13].

To avoid confounding factors, in this study we utilize only the middle coil of the Omnimagnet. Its dipole strength is proportional to its current  $i$  as  $\|\mathbf{M}\| = 6.87i \text{ A}\cdot\text{m}^2$ . We characterized the frequency response of the coil using a Hewlett Packard dynamic signal analyzer (model 35665A). The frequency response in the range of 6–1000 Hz is accurately modeled as a first-order “RL circuit” with a resistance of  $2.19 \Omega$  and an inductance of  $0.089 \text{ H}$ . Using the inverse of this model, we are able to compensate for high-frequency attenuation to ensure that the amplitude of the current generated, and thus the field generated, is invariant to frequency.

The electromagnet is powered by a class D Crown audio amplifier (model XLS 2002), capable of 1050 W of maximum output power for frequencies of 20 Hz to 20 kHz. The frequency response of the amplifier connected to (i.e., loaded by) the coil was measured by the dynamic signal analyzer. The amplifier’s gain was constant at 47.3 (33.5 dB) in the frequency range of 11–10000 Hz.

The amplifier is given an audio signal from a computer running a MATLAB program that creates sinusoidal voltage signals, which are generated by an onboard Realtek sound card (model ALC 887). These sinusoidal signals are fed into the amplifier, which outputs a sinusoidal voltage to the coil. The gain between the commanded MATLAB signal and the measured output voltage from the sound card is 2.44 in the frequency range of 20–250 Hz.

The magnetic field from the electromagnet generates a force  $\mathbf{f} = \nabla(\mathbf{m} \cdot \mathbf{b})$  and torque  $\boldsymbol{\tau} = \mathbf{m} \times \mathbf{b}$  on the stylus’ magnetic dipole  $\mathbf{m}$ , which can be modeled as being at the center of the cubic NdFeB permanent magnet ( $L_m = 12.7 \text{ mm}$ ,

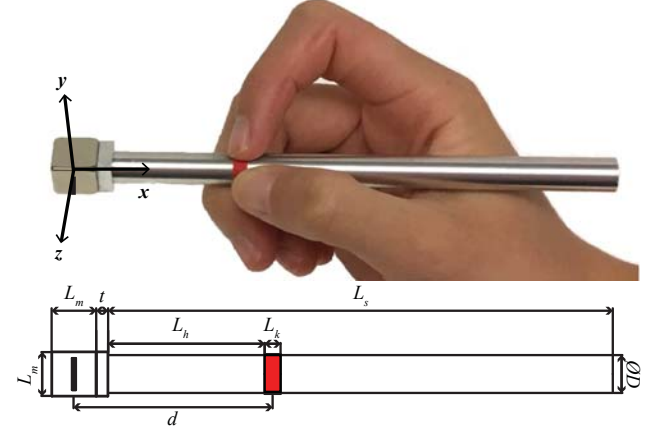


Fig. 1: (Upper) Experimental setup. The untethered magnetic haptic interface comprises an Omnimagnet electromagnetic field source and an untethered magnetic stylus. The subject holds the stylus with a precision grasp with her forearm resting on an armrest, and places the stylus’ magnet at a location indicated by a thin rod extending from the Omnimagnet, without contacting it. Note, the configuration shown corresponds to Fig. 2f. The monitor displays simple prompts. (Middle) Close-up showing posture of a precision grasp. The coordinate system used defines  $y$  as pointing upward, and  $z$  as pointing toward the subject. (Lower) Stylus dimensions.

$\|\mathbf{m}\| = 2.15 \text{ A}\cdot\text{m}^2$ , mass  $m_m = 15.4 \text{ g}$ ). The cylindrical aluminum stylus (mass  $m_s = 25.8 \text{ g}$ , inertia  $I_{xx} = 0.724 \text{ kg}\cdot\text{mm}^2$ ,  $I_{yy} = I_{zz} = 86.4 \text{ kg}\cdot\text{mm}^2$ ) has dimensions  $\varnothing D = 9.53 \text{ mm}$  and  $L_s = 127 \text{ mm}$ , with  $t = 4.00 \text{ mm}$  (this provides a flat surface to attach the permanent magnet). The red band on the stylus ( $L_k = 4.00 \text{ mm}$ ,  $L_h = 31.7 \text{ mm}$ ) indicates the desired resting position of the stylus on the subject’s middle finger. The effective distance between the precision grasp and the haptic interaction point is  $d = 44.1 \text{ mm}$ . The black mark on the permanent magnet indicates the direction of its dipole moment (i.e., pointing from the south pole to the north pole), which is orthogonal to the  $x$  axis.

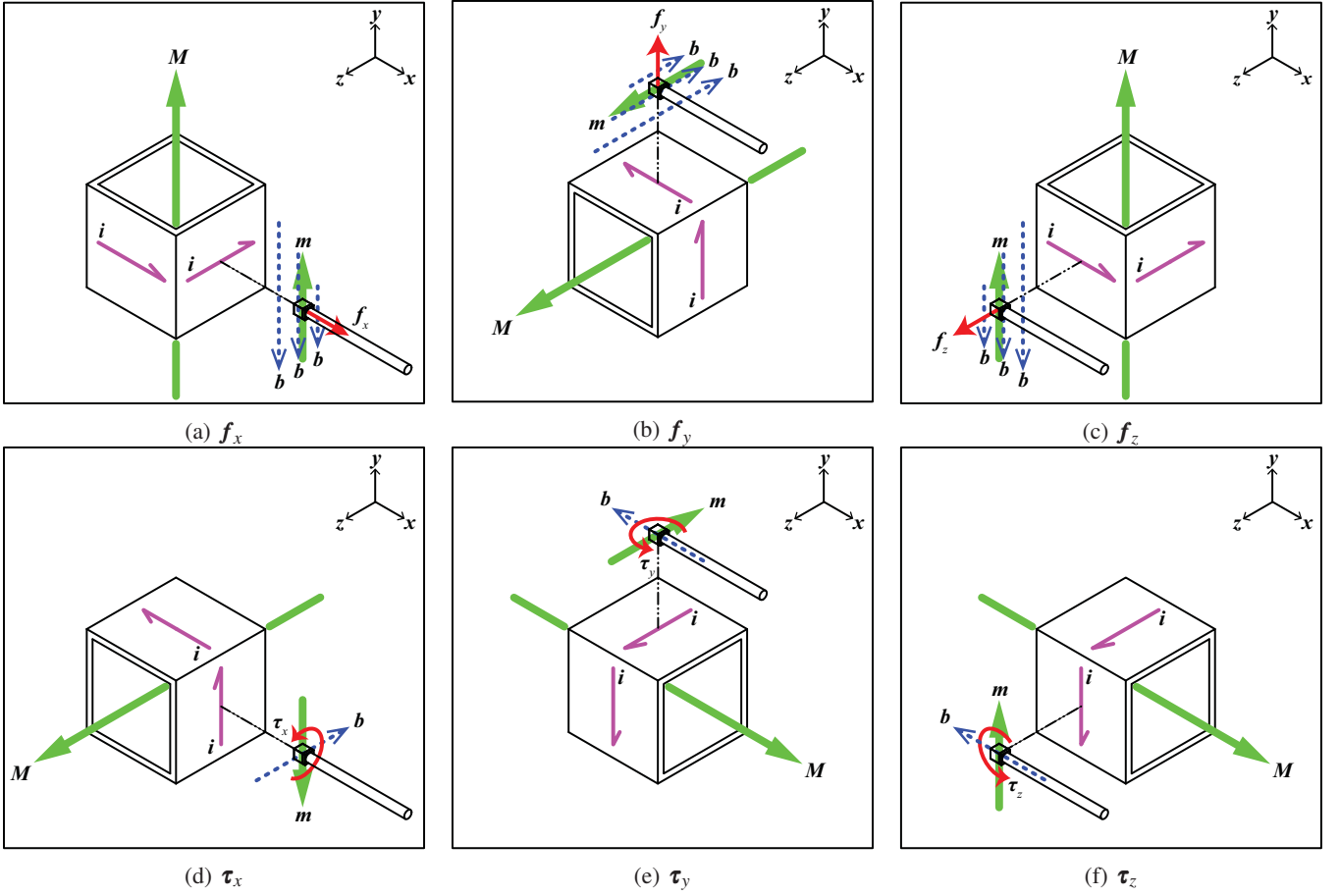


Fig. 2: The six configurations of the untethered magnetic haptic interface used in this study. When current  $i$  flows through the electromagnet as shown, it generates the corresponding dipole moment  $M$  located at the electromagnet's center. The permanent magnet's dipole moment  $m$  is located at its center. The top three configurations correspond to a pure-force mode along a given principal axis, due to the spatial derivative of the field:  $\mathbf{f} = \nabla(\mathbf{m} \cdot \mathbf{b})$ . The bottom three configurations correspond to a pure-torque mode about a given principal axis, as the stylus' dipole attempts to align with the field:  $\boldsymbol{\tau} = \mathbf{m} \times \mathbf{b}$ . When the current is varied sinusoidally in time, the resulting forces and torques vary sinusoidally in time as well.

### C. Design

This experiment uses a full-factorial repeated-measures design with two factors: the configuration of the untethered magnetic haptic interface (Fig. 2) and the frequency of the vibration. We consider six configurations of the untethered magnetic haptic interface, three of which correspond to a pure force along one of the principal axes of the stylus, and three of which correspond to a pure torque about one of the three principal axes. The ten vibration frequencies considered in this experiment are spaced evenly in a base-10 logarithmic scale within the frequency range of 20–250 Hz. This range was chosen because humans are able to detect vibrotactile stimuli in the frequency range of 20–1000 Hz, and most haptic interfaces cannot correctly render vibration beyond 250 Hz [10]; the authors could not perceive the direction of vibration across this frequency range. The above factors yield 60 distinct combinations.

We are interested in determining the absolute threshold of the amplitude (i.e., half peak-to-peak) of the sinusoidal force or torque signal applied to the stylus for each com-

bination. As described in Section II-D, we use an adaptive tracking procedure to determine the vibration threshold of each subject for each combination. This procedure results in a number of reversals, which ultimately leads to six best-estimate-threshold (BET) values for each combination, which are used as repeated measures in the analysis of variance (ANOVA). We use a mixed-effect ANOVA model to determine statistical significance in an experiment with response variable *BET*, blocking factor *subject* treated as a random-effect variable, and treatment factors *configuration* and *frequency* treated as fixed-effect variables. The Tukey post-hoc pairwise comparison test was run for significant factors. The conventional significance for the entire analysis was determined at  $\alpha = 0.05$ , two tailed. All analysis was done with MATLAB R2017b.

We designed our experiment to enable us to investigate three distinct hypotheses: (1) There is a difference in BET between the three principal force modes. (2) There is a difference in BET between the three principal torque modes. (3) There is a notion of “equivalent moment”, via the moment



arm  $d$ , which can be used to equate the thresholds for  $f_y$  and  $\tau_z$ , and for  $f_z$  and  $\tau_y$ .

#### D. Procedure

The experiment is conducted in six sessions, each considering a single configuration and lasting 35–50 minutes per subject. For a given subject, the sessions are separated by at least 48 hours to mitigate the effect of the configuration order [14]. The order of the sessions was randomized for each subject.

At the beginning of a session, the subject sits in front of the table with apparatus on it (Fig. 1). A 100-mm-long thin rod attached to one side of the Omnimagnet indicates the desired position of the stylus. The subject is instructed to rest their forearm on the armrest, hold the stylus using a precision grasp with the center of the middle finger contacting the red band, and place the center of the stylus's permanent magnet close the end of the thin rod without contacting it. Before the experiment begins, the subject is allowed to adjust the height of the chair, the height of the armrest, and the position of the Omnimagnet on the table to facilitate a comfortable precision grasp on the stylus. We note that all six configurations enable the subject to hold the stylus in the same orientation. The subject wears ear muffs for the duration of the experiment to eliminate audio cues from the device and other distractions. A 508 mm (20 inch) monitor, placed at a distance of 686 mm from the subject, provides a visual display.

In a given session, the order of the ten frequencies is randomized for each subject. The subject is given no information about the vibration parameters. The procedure to determine the BET for a given frequency is as follows. A two-interval forced-choice (2-IFC) psychophysical design [15] and a one-up, two-down adaptive tracking procedure [16] is used to determine the BET of the subject for a given frequency. A single 2-IFC trial includes two samples: one sample that does not vibrate the stylus, and one that does, presented in a random order. Each sample lasts 1.5 s with a number “1” or “2” simultaneously displayed on the monitor. Each 2-IFC trial forces the subject to choose which sample had the vibration (whether or not they could perceive one). There is a pause after each trial to allow the subject to indicate, either verbally or with a show of fingers, which sample had the vibration; the response is manually recorded by the experimenter, after which she begins the next trial. The one-up, two-down adaptive tracking procedure determines the amplitude of the vibration signal for each trial. This procedure is started at a high amplitude that is easily felt (determined during pilot testing among the authors), decreased after two successive correct responses, then increased after any single incorrect response, and finally stopped at the 15th reversal. The amplitude is multiplied/divided by 2 for an increase/decrease, respectively, in the first three reversals, and then by  $\sqrt{2}$  in the remaining 12 reversals.

The final 12 reversal amplitudes are used to estimate the threshold for a given frequency, which in turn is the threshold for a given combination. Each reversal amplitude corresponding to a change from increasing to decreasing is paired with

the next reversal amplitude corresponding to a change from decreasing to increasing. The BET for each pair is computed as the geometric mean of the two reversal amplitudes of the pair [17]. Each frequency (i.e., combination) results in six BETs (from the final 12 reversals), which are used as repeated measures in the ANOVA.

After half of the session is complete (i.e., after five frequencies are complete), the subject is forced to take a break of at least 5 minutes to eliminate fatigue. The subject can also take a break at anytime during the session if requested.

### III. RESULTS

#### A. Comparison of Force Thresholds

Figure 3 shows the experimental results for BET, for all frequencies tested, for the three pure-force configurations (Figs. 2a, 2b, and 2c). For all three configurations, there is a clear trend of BET being relatively high (i.e., the subjects are relatively insensitive) at the lowest frequencies, with the BET decreasing with increasing frequency to a minimum value (i.e., frequencies at which the subjects are most sensitive), and then BET increasing with further increases in frequency. A three-way ANOVA with *subject*, *configuration*, *frequency*, and their full interactions for all pure-force configurations (i.e., 30 combinations) shows the effect of *configuration* is statistically significant ( $p < 0.01$ ), as is the effect of *frequency* ( $p < 0.01$ ).

A Tukey post-hoc pairwise comparison test for *configuration* shows the difference between  $f_x$  and  $f_y$  and the difference between  $f_x$  and  $f_z$  are statistically significant ( $p < 0.001$  in each case), but the difference between  $f_y$  and  $f_z$  is not statistically significant.

A Tukey post-hoc pairwise comparison test for *frequency* and *configuration* shows the differences at low frequencies (20–35 Hz) between  $f_x$  and  $f_y$  and between  $f_x$  and  $f_z$  are statistically significant ( $p < 0.001$  in each case), but the differences at all other frequencies and between all other force directions are not statistically significant. BET due to  $f_x$  is significantly higher than due to  $f_y$  and  $f_z$  at low frequencies (20–35 Hz), meaning subjects are less sensitive to force signals parallel to the shaft of the stylus than to force signals orthogonal to the shaft at these low frequencies.

#### B. Comparison of Torque Thresholds

Figure 4 shows the experimental results for BET, for all frequencies tested, for the three pure-torque configurations (Figs. 2d, 2e, and 2f). As with forces, for all three configurations, there is a clear trend of BET being relatively high (i.e., the subjects are relatively insensitive) at the lowest frequencies, with the BET decreasing with increasing frequency to a minimum value (i.e., frequencies at which the subjects are most sensitive), and then BET increasing with further increases in frequency. A three-way ANOVA with *subject*, *configuration*, *frequency*, and their full interactions for all pure-torque configurations (i.e., 30 combinations) shows the effect of *configuration* is statistically significant ( $p < 0.001$ ), as is the effect of *frequency* ( $p < 0.001$ ).

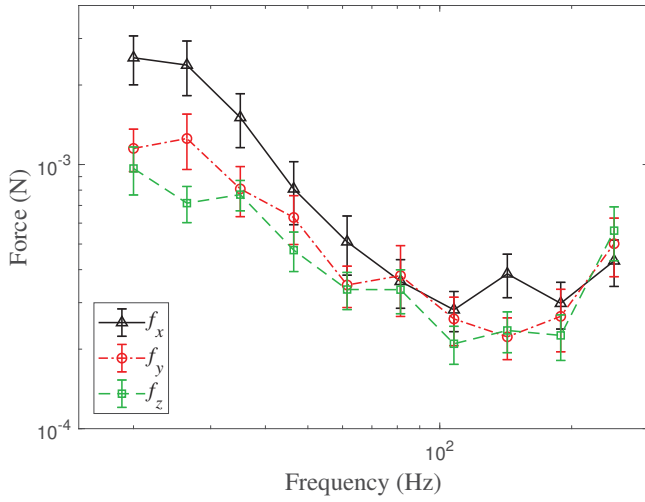


Fig. 3: BET (means with 95% confidence interval (CI)) for the three pure-force configurations, for all frequencies and subjects tested.

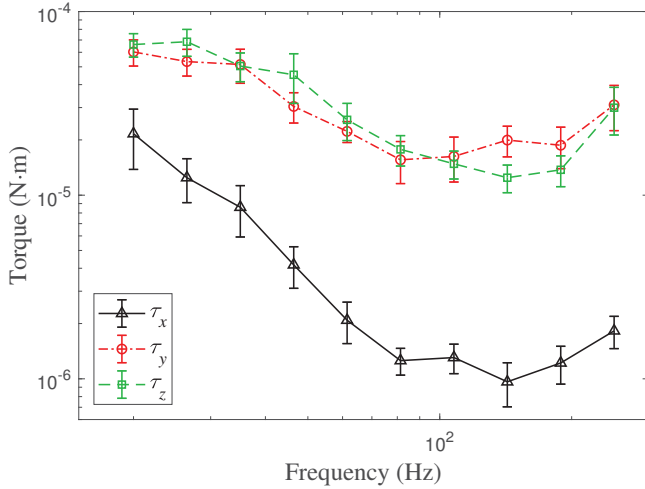


Fig. 4: BET (means with 95% CI) for the three pure-torque configurations, for all frequencies and subjects tested.

A Tukey post-hoc pairwise comparison test for *configuration* shows the difference between  $\tau_x$  and  $\tau_y$  and the difference between  $\tau_x$  and  $\tau_z$  are statistically significant ( $p < 0.001$  in each case), but the difference between  $\tau_y$  and  $\tau_z$  is not statistically significant.

A Tukey post-hoc pairwise comparison test for *frequency* and *configuration* shows that, at all frequencies, the differences between  $\tau_x$  and  $\tau_y$  and the difference between  $\tau_x$  and  $\tau_z$  are statistically significant ( $p < 0.001$  in each case). BET due to  $\tau_x$  is significantly lower than due to  $\tau_y$  and  $\tau_z$  at all frequencies, with a large effect size; the BET means of  $\tau_x$  are approximately three times lower than the BET means due to  $\tau_y$  and  $\tau_z$  at the lowest frequencies, and are approximately 20 times lower at the frequencies of peak sensitivity. This means that subjects are substantially more sensitive to torque signals about the shaft of the stylus than torque signals orthogonal to the shaft.

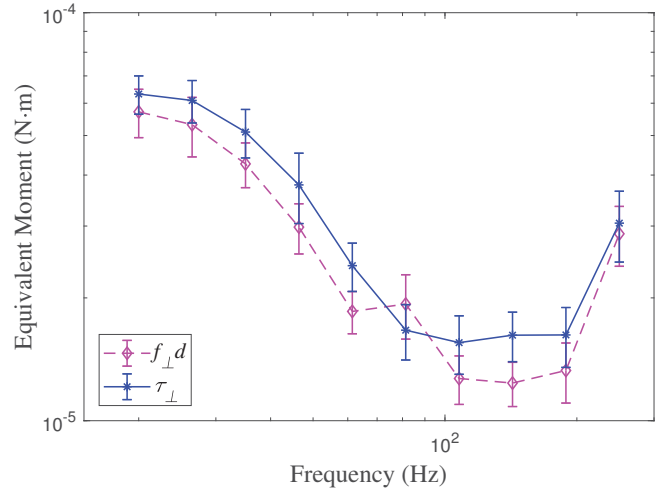


Fig. 5: BET (means with 95% CI) for the pure-torque configuration  $\tau_{\perp}$ , as well as for the pure-force configuration  $f_{\perp}$  multiplied by the distance (i.e., moment arm)  $d$ , for all frequencies and subjects tested.

### C. Comparison of Equivalent-moment Thresholds

When a pure torque  $\tau_{\perp}$  is applied orthogonal to the axis of the stylus, an equal and opposite reaction moment is experienced at the grasp point. We hypothesize that a pure force  $f_{\perp} = \tau_{\perp}/d$  applied orthogonally to the axis of the stylus will have the same BET as that due to  $\tau_{\perp}$ , because it would result in the same reaction moment. We assume the effective distance  $d$  between the HIP and the precision grasp used in our experiment. Based on the results of Sections III-A that suggest that  $f_y$  and  $f_z$  are largely equivalent, we created a new data set,  $f_{\perp}$ , which is the union of all BETs of  $f_y$  and  $f_z$  (each individual BET is used as repeated measures in ANOVA). Similarly, based on the results of Sections III-B that suggest that  $\tau_y$  and  $\tau_z$  are largely equivalent, we created a new data set,  $\tau_{\perp}$ , which is the union of  $\tau_y$  and  $\tau_z$ .

Figure 5 shows the experimental results for BET, for all frequencies tested, for  $\tau_{\perp}$  and  $f_{\perp}d$ . A three-way ANOVA with *subject*, *frequency*, and *configuration*, and their full interactions, but now using our new *configuration* levels of  $\tau_{\perp}$  and  $f_{\perp}d$ , did not find a significant effect of *configuration*. If there is, in fact, a difference between  $\tau_{\perp}$  and  $f_{\perp}d$ , its effect size will likely be small. This suggests that  $\tau_{\perp}$  and  $f_{\perp}d$  are largely equivalent, providing evidence that our equivalent-moment assumption can be applied in practice.

## IV. DISCUSSION

The equivalent-moment conclusion of Section III-C suggests a bridge that enables critical comparison of all six principal modes of vibrotactile display, which use both forces and torques, which have different units and are thus not trivially comparable. For systems in which it is possible to generate vibrotactile signals across multiple degrees of freedom using multiple independent actuators, this result will enable the direction of vibrotactile display to be chosen to efficiently render a desired sensation. However, although

the six principal modes are orthogonal at the HIP, they do not result in fully independent vibrotactile sensations at the grasp, so more work is required to understand how the six principal modes will superimpose [18].

We also note that the equivalent-moment conclusion may not hold for values of  $d$  that are significantly shorter than ours, because the reaction moment felt at the grasp point in an  $f_{\perp}$  mode will decrease with decreasing  $d$ , and the unmodeled reaction forces will become relatively more important.

Because the  $\tau_x$  principal mode is so much stronger than the other torque modes, haptic-interface designers may want to consider this result to provide vibrotactile feedback. In the case of untethered magnetic haptic interfaces, we should attach the permanent magnet on the stylus with  $\mathbf{m}$  orthogonal to stylus  $\mathbf{x}$  axis, because with  $\mathbf{m}$  aligned with the  $\mathbf{x}$  axis it would not be possible to generate any magnetic torque about the stylus. In the case of six-degree-of-freedom impedance-type haptic interfaces, using only the actuator designed to apply torque about the stylus  $\mathbf{x}$  axis could be an effective way to decouple vibrotactile display from the kinesthetic display, potentially even by superimposing a audio-amplifier signal on the kinesthetic signal generated by the haptic interface's native control system. In the case of haptic interfaces driven by vibrotactile actuators, prior work [9] made a good choice of attaching a force-type vibrotactile actuator to a stylus such that vibrations are orthogonal to the stylus  $\mathbf{x}$  axis, as opposed to aligned with the  $\mathbf{x}$  axis.

In all six modes we observe peak sensitivity in the range of 100–200 Hz, which is consistent with other works using a stylus [6], [10]. The results that subjects are relatively less sensitive in the  $f_x$  mode using a precision grasp is consistent with Brisben's conclusion, using a power grasp, that vibration parallel to the skin surface is easier to detect than vibration perpendicular to the skin [11].

The overall trend of the  $f_x$  mode that we observed is similar with the force-threshold curve for the same mode reported in [6]. They report a threshold of 21 mN amplitude at 20 Hz, whereas we measure 2.5 mN amplitude at the same frequency, seeming to suggest that subjects were substantially more sensitive in our study in this low-frequency region. However, their minimum threshold was found at 160 Hz, with an amplitude of 66  $\mu$ N; whereas our minimum threshold was found at 108 Hz, with an amplitude of 282  $\mu$ N (with a similar value at 189 Hz), seeming to suggest that subjects were substantially less sensitive in our study in this peak-sensitivity region. There are a number of differences between our study and [6] that could explain the differences observed. Their stylus is oriented vertically, which puts the subject's wrist into a different posture. The weight of their stylus is gravity compensated. Finally, their force is measured with a force sensor sandwiched between a shaker and an accelerometer that is rigidly attached to the stylus, and the dynamics of the two sensors may affect the results. However, it is unlikely that any discrepancies in absolute values will affect the relative hierarchy of the six principal modes reported here.

## V. CONCLUSION

This study characterized the vibrotactile detection thresholds in the frequency range of 20–250 Hz of ten human subjects holding a stylus with a precision grasp. For the first time, we considered all six principal modes of vibrotactile display rendered at the haptic interaction point of the stylus, which includes three orthogonal force directions and three orthogonal torque directions. We found that subjects are far more sensitive to torque signals about the shaft of the stylus than to torque signals orthogonal to the shaft. We found that, at low frequencies, subjects are less sensitive to force signals parallel to the shaft of the stylus than to force signals orthogonal to the shaft. Finally, we found that the thresholds for force and torque signals applied orthogonal to the shaft of the stylus can be approximately equated by considering the reaction moment felt at the grasp point, which enables all six principal modes to be quantitatively compared.

## REFERENCES

- [1] M. C. Lin and M. Otaduy, *Haptic rendering: foundations, algorithms, and applications*. CRC Press, 2008.
- [2] B. Hannaford and A. M. Okamura, "Haptics," in *Springer Handbook of Robotics*. Springer, 2016, pp. 1063–1084.
- [3] J. R. Napier, "The prehensile movements of the human hand," *Bone & Joint Journal*, vol. 38, no. 4, pp. 902–913, 1956.
- [4] J. B. Brink, A. J. Petruska, D. E. Johnson, and J. J. Abbott, "Factors affecting the design of untethered magnetic haptic interfaces," in *Proc. IEEE Haptics Symposium*, 2014, pp. 107–114.
- [5] S. Choi and K. J. Kuchenbecker, "Vibrotactile display: Perception, technology, and applications," *Proc. IEEE*, vol. 101, no. 9, pp. 2093–2104, 2013.
- [6] A. Israr, S. Choi, and H. Z. Tan, "Detection threshold and mechanical impedance of the hand in a pen-hold posture," in *Proc. IEEE/RSJ Int. Conf. Intelligent Robots and Systems*, 2006, pp. 472–477.
- [7] J. Bell, S. Bolanowski, and M. H. Holmes, "The structure and function of pacinian corpuscles: A review," *Progress in Neurobiology*, vol. 42, no. 1, pp. 79–128, 1994.
- [8] R. Lundström, "Local vibrations/mechanical impedance of the human hand's glabrous skin," *Journal of Biomechanics*, vol. 17, no. 2, pp. 137 141–139 144, 1984.
- [9] H. Culbertson, J. Unwin, and K. J. Kuchenbecker, "Modeling and rendering realistic textures from unconstrained tool-surface interactions," *IEEE Trans. Haptics*, vol. 7, no. 3, pp. 381–393, 2014.
- [10] A. M. Okamura, M. R. Cutkosky, and J. T. Dennerlein, "Reality-based models for vibration feedback in virtual environments," *IEEE/ASME Trans. Mechatronics*, vol. 6, no. 3, pp. 245–252, 2001.
- [11] A. Brisben, S. Hsiao, and K. Johnson, "Detection of vibration transmitted through an object grasped in the hand," *J. Neurophysiology*, vol. 81, no. 4, pp. 1548–1558, 1999.
- [12] A. J. Petruska and J. J. Abbott, "Omnimagnet: An omnidirectional electromagnet for controlled dipole-field generation," *IEEE Trans. Magnetics*, vol. 50, no. 7, 2014.
- [13] A. J. Petruska, J. B. Brink, and J. J. Abbott, "First demonstration of a modular and reconfigurable magnetic-manipulation system," in *IEEE Int. Conf. Robot. Autom.*, 2015, pp. 149–155.
- [14] H. R. Dinse, P. Ragert, B. Pleger, P. Schwenkreis, and M. Tegenthoff, "Pharmacological modulation of perceptual learning and associated cortical reorganization," *Science*, vol. 301, no. 5629, pp. 91–94, 2003.
- [15] D. M. Green, "Stimulus selection in adaptive psychophysical procedures," *J. Acoust. Soc. Am.*, vol. 87, no. 6, pp. 2662–2674, 1990.
- [16] H. Levitt, "Transformed up-down methods in psychoacoustics," *J. Acoust. Soc. Am.*, vol. 49, no. 2B, pp. 467–477, 1971.
- [17] M. C. Meilgaard, B. T. Carr, and G. V. Civile, *Sensory evaluation techniques*. CRC press, 2006.
- [18] N. Landin, J. M. Romano, W. McMahan, and K. J. Kuchenbecker, "Dimensional reduction of high-frequency accelerations for haptic rendering," in *Proc. Int. Conf. Human Haptic Sensing and Touch Enabled Computer Applications*. Springer, 2010, pp. 79–86.